Innovations in single photon emission computed tomography

M.S. Maxim Antakov, Igor Burnaevsky

March 20-27 2011, Moscow
JASS 2011

1. Introduction

Single photon emission computed tomography (SPECT, or less commonly, SPET) is a nuclear medicine tomographic imaging technique using gamma rays. However, it is able to provide true 3D information. This information is typically presented as cross-sectional slices through the patient, but can be freely reformatted or manipulated as required. Myocardial perfusion scan is a nuclear medicine procedure that illustrates the function of the heart muscle (myocardium). It evaluates many heart conditions from coronary artery disease to hypertrophic cardiomyopathy and myocardial wall motion abnormalities. The function of the myocardium is also evaluated by calculating the left ventricular ejection fraction of the heart. This scan is done in conjunction with a cardiac stress test.

Because blood flow in the brain is tightly coupled to local brain metabolism and energy use, technetium tracer is used to assess brain metabolism regionally, in an attempt to diagnose and differentiate the different causal pathologies of dementia. Meta analysis of many reported studies suggests that SPECT with this tracer is more sensitive at diagnosing Alzheimer's disease vs. clinical exam (mental testing, etc.).

2. Using of MMS

The main purpose of using multiplexed measurement systems is to replace huge, complicated and expensive rotating diagnostic scheme by simple and chip translational scheme. Such diagnostic scheme can also be applied in cases, where rotation around object is impossible.

Lens is used in optics to obtain the image of the radiating object. But it can't be used in case of the ionizing radiation because such kind of radiation does not refract.

However, another method for obtaining images is use of obscura-chamber. This method can be also used for ionizing radiation. Image of flat radiating object, which is obtained on the position sensitive detector, is inverted image of source.If we replace the flat source by the volume source, the image on the detector will be a superposition of images of each plane of a source. Thus, such kind of image is impossible to restore.

3. Construction of MMS

If we replace single pinhole by a set of opened and closed pinholes, we will receive, so-called, coded aperture. It has focus properties, so they make it some analog of lens. Thus even for a point source of the radiation which locates in a focal plane, on the detector we will obtain difficult image representing a shade of a aperture. Image decoding is required. In a case of a non-flat source the image on the detector is even more difficult.

There are three methods to construct 2-D code table from 1-D sequences. Line-by-line and diagonal methods construct 2-D CT on the basis of one PRS. Self-supported method constructs 2-D CT on the basis of two PRS.

4. Focal plane method

To reconstruct the view of space distribution of radiating source focal planes method is used. Volume source is divided into planes, which sequentially placed in focus of system MPCA-PSD. Obtained images on the detector are used in inversed algorithm of decoding.

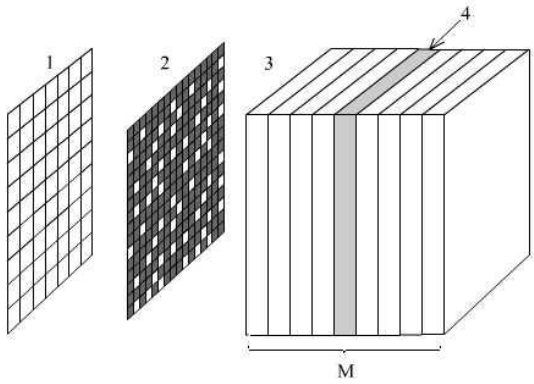

Fig. 1. Focal plane method: *1* –Position-sensitive detector (PSD), *2* – coded aperture, *3* – space distributed source,
4 –focal plane

There is known algorithm to decode flat source. Using this algorithm in case of the volume source can obtain so-called focused images. At the same time the focused image may be used as the initial approximation

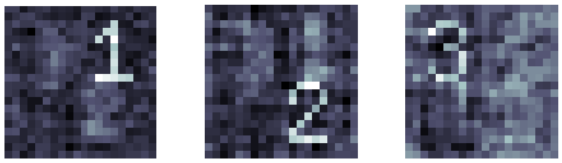

Fig. 2. Focused images in case of 3 planes

5. Back projection algorithm

There are known iterative algorithms, for example, steepest descent method, directed divergence method.

But they showed their extreme inefficiency, so it is actual to create an iterative algorithm based on the back projection, which shall have the significantly better rate of the convergence. At the same time, it is known that in the transaxial rotational tomography there are very effective algorithms of ART-type for solution of the reconstruction problem. The ART-type algorithms use the idea of the back projection.

Back projection method (BPM) is developed on the basis of an idea of back projecting. The basis of BPM is a priori information about contributions, which sources can contribute to every cell of PSD (Fig. 3). Iterations in BPM are performed in accordance with the formula:

$$\vec{s}^{(k+1,1)} = \vec{p}^{(k)}, \quad (1)$$

$$\vec{s}^{(k+1,i)} = \vec{s}^{(k+1,i-1)} + \frac{q_i - \vec{h}_i^{\top}\vec{s}^{(k+1,i-1)}}{\vec{h}_i^{\top}\vec{h}_i}\vec{h}_i, \quad i = 2,3,\ldots, Mv, \quad (2)$$

$$\vec{p}^{(k+1)} = \vec{s}^{(k+1,Mv)}, \quad (3)$$

Back projection method has only one disadvantage – it is requires much computational time.

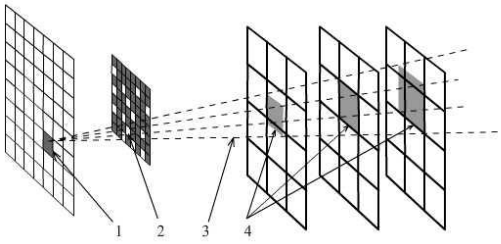

Fig. 3. Back projection method: *1* – PSD cell, *2* – open pinhole, *3* – back projection cone, *4* – source cells, which contained in cone

Initial and subsequent approximations can be characterized by mean-square, absolute and maximum deviations of the reconstructed image from the real image, respectively:

$$\begin{cases} D = \sqrt{\frac{1}{Mv}\sum_i\sum_{j=1}^{v}(\tilde{\xi}_j^i - \xi_j^i)^2}, \\ R = \frac{1}{Mv}\sum_i\sum_{j=1}^{v}|\tilde{\xi}_j^i - \xi_j^i|, \\ E = \frac{1}{M}\sum_i\frac{1}{v}\max_{j\in[1,v]}\{\tilde{\xi}_j^i - \xi_j^i\}. \end{cases} \quad (4)$$

To investigate the quality of the proposed iterative algorithm for reconstruction of the space distribution of radiation sources numerical experiments were carried out. Modeled source was set of 9 planes. In each plane source looks like smiles, which locates in different places of the plane. The maximum value of the source is 1, the minimum value of the source is 0. SDM (Fig. 4b) and DDM (Fig. 4c) converges much slower then BPM (Fig. 4d) as it may be visually seen. Quantitative data are shown in Fig. 5, which show the criteria (4) dependences on the number of iterations for the SDM, DDM and BPM. Numerical experiments were carried out for different types of coded apertures. It was found that the use of BPM as well as SDM and DDM is more effective for coded apertures with a small average transparency.

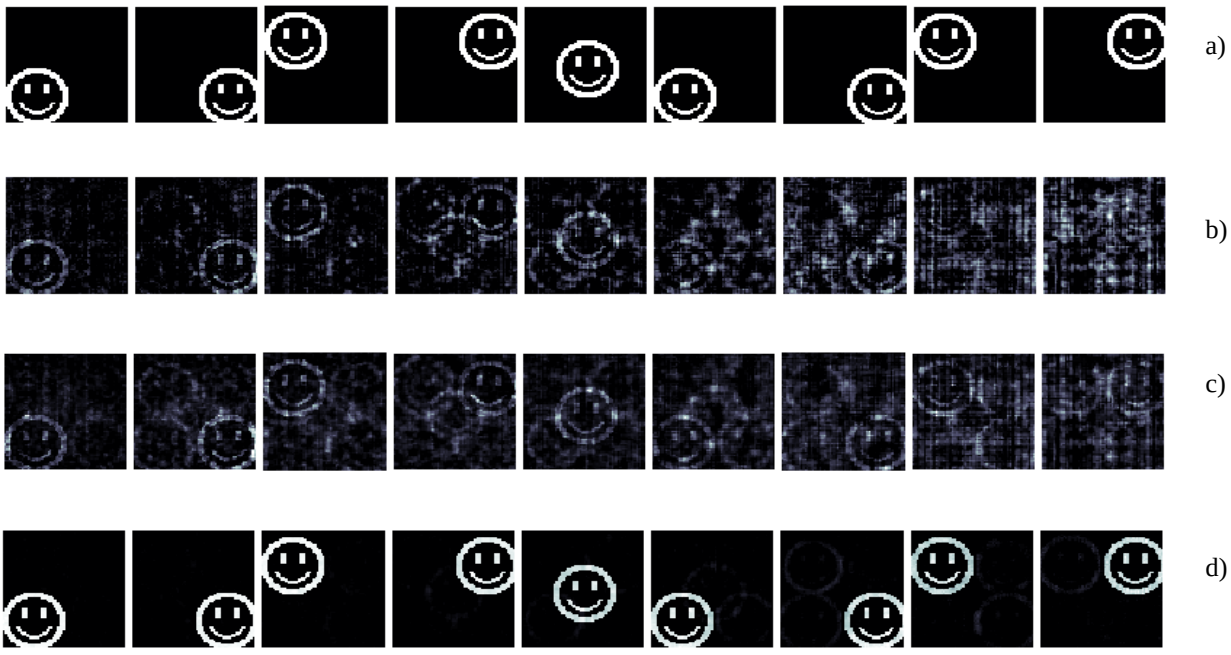

Fig. 4. The real (a) and obtained images of test source after 25 iterations for SDM (b), DDM (c) and BPM (d).

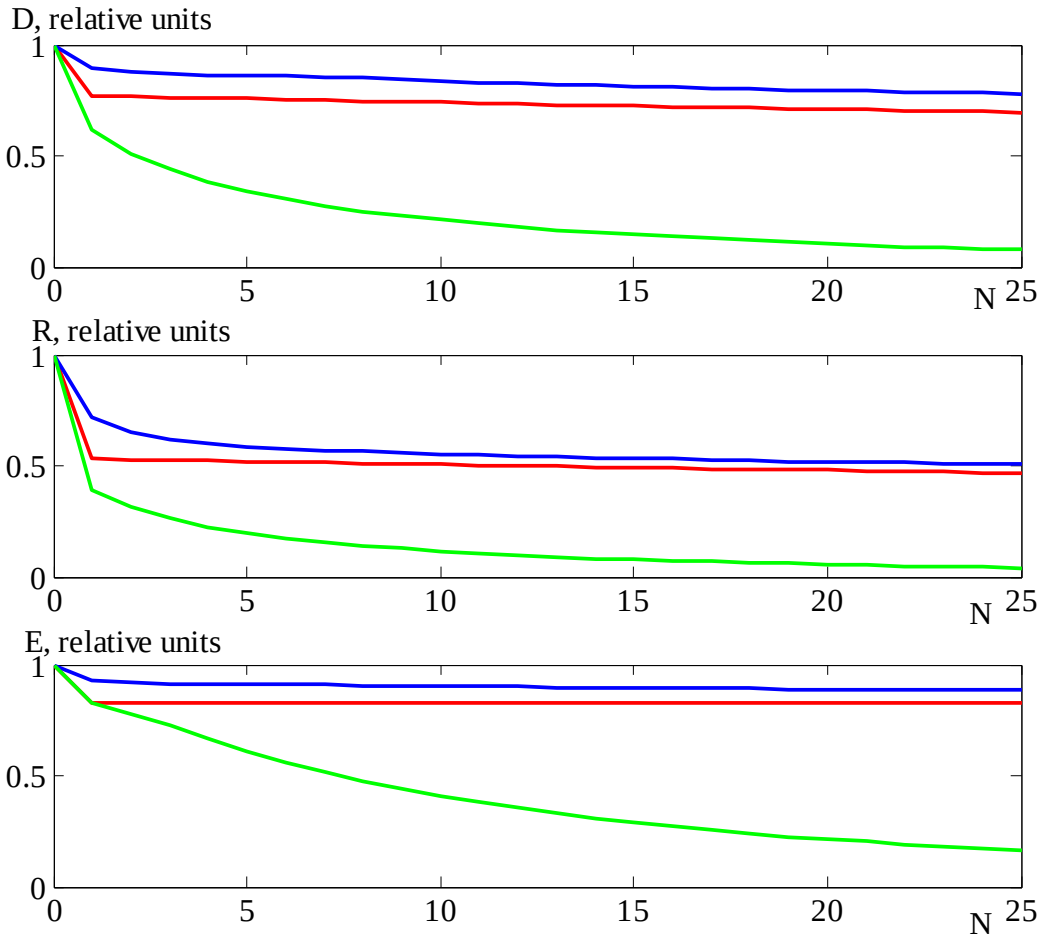

Fig. 5. Dependences of criteria of the closeness of the reconstructed and the true source on the number of iterations for the SDM (blue line), DDM (red line) and BPM (green line).

6. Bipolar measurement scheme

Shown before scheme called unipolar. This means that we focus on the investigated plane only from one side. However, we can double the amount of data, if we will focus on the investigated plane from two sides. Such a measurement scheme is called bipolar. It can be used with the same or different coding apertures. Using this measurement scheme averages volume decoding error.

Simple bipolar measurement scheme can be easily implemented with the one device working by a unipolar scheme. Thus it is enough to turn the test object at 180 degrees.

In X-ray transmission tomography for testing usually use the Shepp-Logan phantom, which simulates the complex spatial distribution of absorption coefficient. In emission tomography we can use similar phantom which simulates the complex spatial distribution of radiation sources. Visually, phantom is a superposition of ellipsoids with different orientation. Within each ellipsoid emission intensity has a constant activity. In areas of overlap ellipsoids source activity is the sum of all the activities of overlapping ellipsoids. Reconstruction with the bipolar measurement scheme significantly improves the image quality.

The degree of improvement can be traced by the dependence of the standard deviation of the iteration number. It was found that the rate of deviation reduction for the bipolar measurement scheme more than for unipolar scheme is about 10 times.

Thus a bipolar measurement scheme can be used for a large number of planes. On the slide shows the Shepp Logan phantom reconstruction using back projection method after only 5 iterations. (Fig. 6).

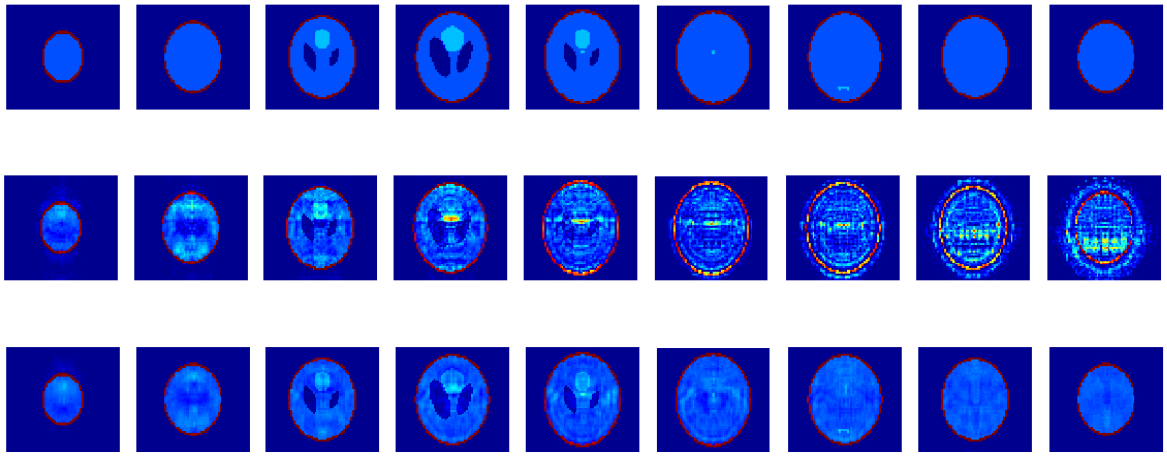

Fig. 6. The real (a) and obtained images of test Shepp-Logan source after 5 iterations for BPM working on the unipolar (b), and bipolar (c) scheme.

7. Hexagonal coded apertures

In addition to the rectangular configuration of coding devices, which we saw earlier, they can also be used in other configurations. Hexagonal configuration of coding devices are widespread in X-ray astronomy. Position of open and closed pinholes in them as well as in rectangular CA defined by the position of 1 and 0 in the pseudo-random sequence, which is specially rolled into a hexagonal configuration. In this case, the length of the PRS imposed the condition:

$$V = 3R(R+1)+1, \qquad (5)$$

where the parameter R is called the rank of the HCA.

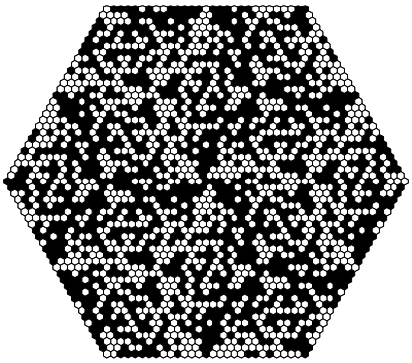

Fig. 7. Hexagonal coded aperture

We have modified decoding algorithms of detector readings in the case of a hexagonal configuration, and have achieved that in the case of a planar source, there is absolutely accurate decoding. As expected, the volume source, even in the case of two planes, in decoding artifacts appear due to the influence of non-focal planes.

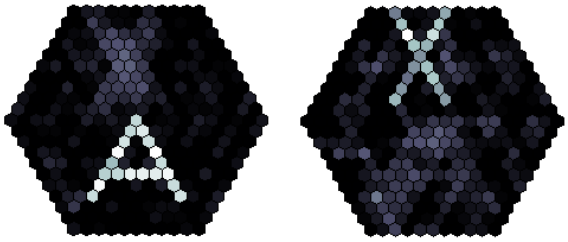

Fig. 8. Focused images in case 2 planes

To analyze the value of those contribution as well as for rectangular configurations usually use the concept of point spread function. To determine PSF of the coded aperture space of the volume source is divided into cells. For each cell contribution of this cell in the image in the focal plane is computed. Consequently we have a set of PSF which are describe current coded aperture. Whole set of PSF can be characterized by the top, the bottom, and the medium.

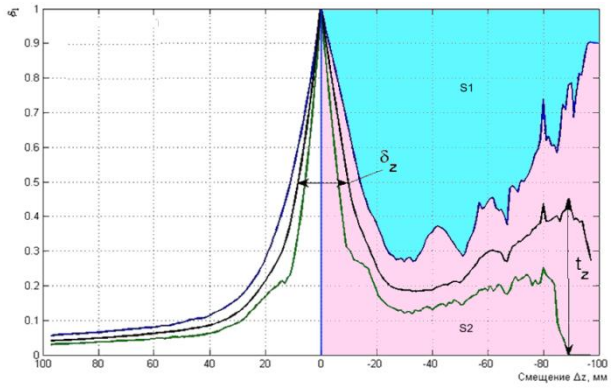

Fig. 9. Point-spread function for hexagonal coded aperture with rank 25

On the right side of the apparatus function observed nonmonotonic (false peaks), And bigger they are, the worst coded aperture is. PSF can be characterized by the full width at the half maximum (FWHM) and by the maximum of the magnitudes of false peaks.

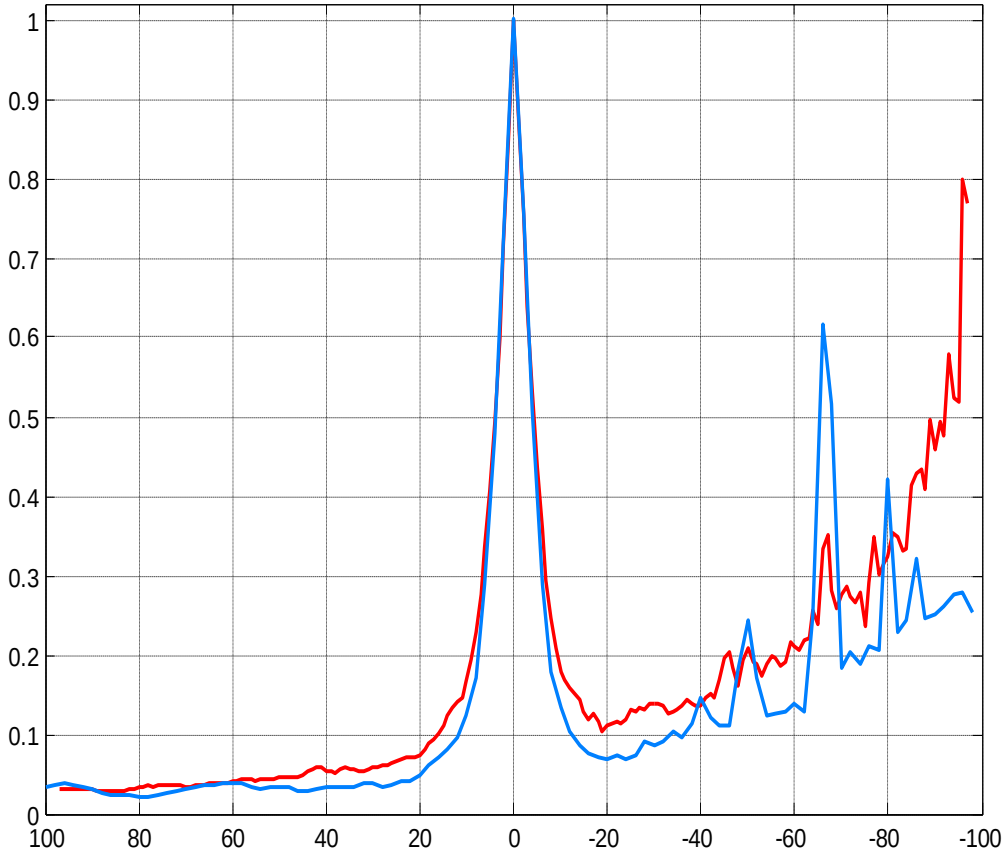

Fig. 10. Point-spread functions for hexagonal coded aperture (blue line) and rectangular (red line) with similar number of pinholes, and average transparency.

On the Fig.10 shows two PSF for square and hexagonal coding devices with similar number of pinhole. In the case of the hexagonal configuration of the false peaks at offsets -50, -66, -80 mm higher, but the average the whole PSF is below. This suggests that the contribution of nonfocal planes for a HCA on average, less than a square

8. Conclusions

Single photon emission computed tomography is one of the most intelligent and promising diagnostic procedure.

Using multiplexed measurement systems allows to replace rotating motion by the translating motion, which also can be applied when rotating around object is impossible

Bipolar measurement scheme double number of measurements but more than five times decrease mean-squared deviation in the iterative algorithms

Using hexagonal coded apertures is new and promising direction of the MMS development

9. References

[1] Caroly J, Stephen J.B., Di Cocco G. et al. Coded aperture imaging in X-and Gamma-ray astronomy. Space Science Reviews, 1987, vol. 45, Nos. 3/4, P. 349-403.

[2] Fedorov G. A., Tereshchenko S. A. // Measurement Techniques. – 2001, №4, P. 57-60.

[3] Fedorov G. A., Tereshchenko S. A. // Measurement Techniques. –2007. – V. 50. – N 6. – P. 681.

[4] Fedorov G. A., Tereshchenko S. A., Antakov M.A. // Measurement Techniques. – 2010. – №3. – P. 47-51. [In Russian]

[5] Fedorov G.A., Tereshchenko S.A. Computed emission tomography. M.: Energoatomizdat, 1990. [In Russian]

[6] Fedorov G.A. Radiation introscopy: Coding of information and optimization of the experiment. M.: Atomizdat, 1982. [In Russian]

[7] Gordon R. A tutorial on ART. (Algebraic reconstruction techniques) //IEEE Tr. on Nuclear Sciences, 1974. – V. NS-21, No. 1. – P. 78–93.

[8] Harwit M., Sloane N.J.A. Hadamard transform optics.– New-York, Academic Press, 1979.

[9] Makuilyams F.J., Sloan N.J. – TIIER, 1976, v.64, №12. P.80. [In Russian]

[12] Spann P.– TIIER, 1965, v.53, №12. P. 2363. [In Russian]

[13] Tereshchenko S.A. Methods of computed tomography. M.: Fizmatlit, 2004. [In Russian]

[14] Wilhelmi G., Gompf F.– Nucl. Instr. Meth., 1970, v.81, N1. p. 36.